MODELLING OF ACTIVITY OF MnO IN FERROMANGANESE AND SILICOMANGANESE SLAGS BY NEURAL NETS

Hakan Cengizler*, Rauf Hurman Eric* and Markus Reuter#

* School of Process and Materials Engineering, University of the Witwatersrand, Johannesburg, Private Bag 3, WITS 2050, South Africa, +27 11 716 2580

\# Faculty of Mining and Petroleum Engineering, Delft University of Technology, Delft, The Netherlands.

ABSTRACT

Gas equilibration technique was used to determine the activity of MnO at 1500°C in synthetic CaO-MgO-SiO_2-Al_2O_3-MnO slags that are typically encountered in submerged arc furnaces. The activity of Mn in Pt-Mn alloys was also measured at 1500°C which confirmed earlier results of strong negative deviations. This data was employed in calculating the activity of MnO in equilibrated slag samples. The experimental MnO activity data on synthetic slags was modelled by the use of neural nets (NN). In this work the applied multi-layer feed forward NNs were trained by a conjugate-gradient optimisation for which a three layer formulation was used. Very good fits were obtained. Activity of MnO was found to increase with increasing concentration of MnO, basicity ratio and CaO/MgO ratio.

1. INTRODUCTION

1.1 Neural Nets

Lippmann[1] discussed various NN-topologies such as Hopfield nets, Hamming nets, Carpenter/Grossberg classifiers etc. For the purpose of this paper the applied multilayer feedforward NNs are not trained by back propagation (BP) using the generalized delta rule (GDR)[2], but by a conjugate-gradient optimization[3,4] procedure similar to that proposed by Barnard and Cole[5]. According to these authors the heuristic algorithms for choosing the learning rate and momentum term (parameters in the GDR algorithm) cannot compete with optimized conjugate-gradient training as far as speed and robustness are concerned.

A neural net is capable of learning the non-linear functional relationship existing between a set of inputs and outputs[6]. In this capacity the neural net is used to determine the functional relationship that exist between N dependent and independent variables, which characterize the system under consideration. For a three layer neural net[1] the following function may be formulated, which relates x_i inputs to the output y_o from node o:

$$y_o = \sum_h \left(\frac{A_{oh}}{1 + e^{-\left(\sum_i B_{hi} \cdot x_i + C_h \cdot 1\right)}} \right) \quad (1)$$

where **h** is number of nodes in the hidden layer, **i** is number of input nodes and **o** is number of output nodes.

This functional relationship, representing the neural nets used for examples in this paper in which all hidden nodes are sigmoidal, implies that the input x_h to the hidden node h is given by

$$x_h = \sum_i (B_{hi}.x_i + C_h.1) \quad (2)$$

since input nodes have linear activation functions, and the output y_h from hidden node h is given by

$$y_h = \frac{1}{1+e^{-x_h}} \quad (3)$$

since these have sigmoidal activation functions[7,8].

During training the weights A_{oh} (*weight between output (o) and hidden (h) nodes)*, B_{hi} (*weight between hidden (h) and input (i) nodes*) and C_h (*weight between hidden (h) and bias node*) are determined. This is effected by presenting the neural net a training data set and following a training algorithm based on conjugate gradient optimization (*algorithm alternates between Polak-Ribiere and Fletcher-Reeves[4] as dictated by certain set tolerances in the programme*) and restart procedures. Other activation functions for the hidden nodes such as linear inverse, exponential, logarithmic, parabolic and hyperbolic, are also accommodated, this architecture showing a similarity with the non-parametric regression projection pursuit method proposed by Friedman[9]. The objective function that is minimized during neural net training is :

$$E = \frac{1}{2}. \sum_o \sum_n (y_o - y_{o,exp})^2 \quad (4)$$

After having trained the neural net, the degree of generalization possible with the net may be tested by the test data set, which is a subset randomly selected from the total data set. It is also possible to test the trained neural nets by statistical methods such as the final R^2 (*square of regression coefficient*), S (*standard deviation*), DF (*degrees of freedom*), x^2 (*Chi^2-probability*) and a measure of overfitting is given by the final prediction error (FPE).

$$FPE = \frac{E}{N}.\frac{(1+w/N)}{(1-w/N)} \quad (5)$$

where **E** is the least square error, which is also the objective function of the conjugate gradient optimization procedure applied here for training the NNs, w are the parameters or neural net weights {=(1+o+i).h} and **N** the total number of data sets.

As a theoretical example a training data set consisting of 18 data points ($0 \leq x \leq 10$) produced by the simple exponential equation $y = e^{-x}$ was used to train a three layer neural net with two linear input nodes, of which one is the bias node (input = 1), three sigmoidal hidden nodes and one linear output node. Trained net statistics are R^2. = ca. 1, S ca. 10^{-5}, DF = 9, x^2- probability = 0.034, FPE ca. 10^{-9} for a net architecture 1 input (linear), 1 output (linear) and 3 hidden (sigmoidal) nodes. If one of the sigmoidal hidden nodes is replaced by an exponential node, FPE decreases to ca. 10^{-16}, improving the predicted accuracy to the 9th decimal. The resulting equivalent neural net function for three sigmoidal hidden nodes is given by eq. 6.

$$y = \frac{0.7032241}{1+e^{-(-0.2012817-1.6963985.x)}} +$$

$$+ \frac{0.9947717}{1+e^{-(-0.0499753-0.9909904.x)}} +$$

$$+ \frac{1.7781301}{1+e^{-(-2.0730975-2.5918490.x)}} \quad (6)$$

The degree of correspondence between test data and predictions by the trained neural net for these data is an indication of the generalization possible by this net (eg. for x=1 (training value) the trained neural net produces 0.367873 for a theoretical vale of 0.367879 and for x = 3.75 (untrained value) the net gives 0.02350 for a theoretical value of 0.02351). Similar nets can be defined for other functions to demonstrate that the functional form of eq. 6 may be applied to approximate these.

1.2 The Slag System

The slag system of CaO-MgO-SiO_2-Al_2O_3-MnO is of simultaneous interest in the production of both ferromanganese and silicomanganese. In order to increase the efficiency of the smelting process, accurate activity data is essential. A substantial amount of data is available on the binary SiO_2-MnO system[11,12] and on MnO activities in blast furnace type slags and in CaO-SiO_2-MnO and MgO-SiO_2-MnO ternary systems[13-23]. In complex systems similar to ferromanganese slags, one study[24] has been carried out on slags with higher basicities than those used in the present investigation. The findings of this study[24] indicated that - within the compositional limits of the study - an increase in the concentration of MnO in the slag, increased its own activity coefficient. On the other hand an increase in the Al_2O_3 content for a given basicity ratio decreased the activity coefficient of MnO especially in highly basic slags.

2. EXPERIMENTAL PROCEDURE

The gas equilibration technique was used for the determination of activity composition relations both in Pt-Mn alloys and in slags. A gas tight vertical furnace heated electrically with molybdenum wire as the resistance was used. The ancillary equipment involved gas-purification train and a gas mixer of conventional design utilizing capillary tubes connected to flowmeters. The equilibrated samples were quenched by dropping them into water contained in a pyrex glass fitted to the bottom end of the recrystallized alumina work tube. Type B thermocouples were employed both for measurement of sample temperatures and for control of furnace temperature. In total, 55 slag samples of different compositions were prepared from reagent grade pure oxides. These synthetic slags had the following initial compositional ranges given in mass percentages :
MnO : 5 - 40% (increasing in 5% steps), CaO : 4 - 35%, MgO : 0.3 - 38%, SiO_2 : 25 - 60% and Al_2O_3 : 2.5 - 7.0%. Using these a total of around 200 successful experiments were conducted. All the oxides, except MnO were first calcined in a muffle furnace at 1200°C for 24 hours. After cooling, the oxides, namely CaO, MgO, Al_2O_3 and SiO_2 were mixed in the desired proportions. the mixtures were pelletized and then homogenized at 1200°C for 12 hours. On cooling, the pellets were crushed and ground in an agate mortar and mixed with the required quantities of reagent-grade MnO before each run. All the mixing procedures were carried out under acetone. The method adopted for the measurement of activities was similar to that used by Abraham et al[13]. platinum strips of dimensions 4mm by 4mm with a thickness of 0.025mm were equilibrated with slag (or pure MnO in the case of activity measurements on Pt-Mn alloys) in a platinum crucible presaturated with respect to manganese. The partial pressure of oxygen was controlled by mixing CO and CO_2 gases; their flow being monitored by capillary tubes connected to flowmeters. If pure MnO is used for equilibration :

$$MnO = \underline{Mn} + 1/2\ O_2(g) \qquad (7)$$

The equilibrium constant will be

$$K = a_{Mn}\sqrt{P'_{O_2}}/a'_{MnO} \qquad (8)$$

When K is known, and $P'o_2$ is controlled, from a knowledge of a'_{MnO}, the activity of Mn in Pt-Mn alloys can be obtained.

When a slag is used in the equilibration experiments, the equilibrium constant will be :

$$K = a_{Mn} \sqrt{Po_2} / a_{MnO} \qquad (9)$$

Since the K values are the same, activity of MnO in slags will be

$$a_{MnO} = \sqrt{Po_2 / P'o_2} \cdot a'_{MnO} \qquad (10)$$

Therefore, Po_2 is the partial pressure of oxygen controlled during a slag experiment, $P'o_2$ is the partial pressure of oxygen that would be in equilibrium with pure MnO and an alloy that contains the same amount of manganese as was formed in the slag experiment, and a'_{MnO} is the activity of the stoichiometric MnO in the non-stoichiometric oxide that would be in equilibrium with $P'o_2$. In the present work $P'o_2$ values were generated together with a_{Mn} values during experiments on the Pt-Mn system. The a'_{MnO} values corresponding to the $P'o_2$ values were obtained form the work of Davies and Richardson[25]. The standard state for MnO activities was changed to pure hypothetical liquid MnO at 1500°C. Preliminary experiments were carried out to determine the equilibrium time, and it was found that the equilibrium was reached within 10 hours in Pt-Mn system and within 6 hours in slag system at 1500°C. To ensure that equilibrium is reached, actual experiments were allowed to proceed for 12 hours. Concentration profiles for manganese on platinum strips obtained by SEM-EDAX combination supported by chemical analysis confirmed that equilibrium had been obtained. Compositional information on slags were obtained by means of the x-ray fusion method done at the Council for Mineral Technology (Mintek) of South Africa.

3. RESULTS AND DISCUSSION

3.1 Activity composition relations in Pt-Mn system

Activity composition relations in the solid solution region of the Pt-Mn binary were determined at 1500°C by the procedure explained earlier. The partial pressure of oxygen in these experiments varied from about 5×10^{-11} to 5×10^{-6} atm. For simplicity a linear-regression model was derived with a correlation coefficient of $r^2 = 0.949$ for the activity coefficient of manganese within the solid solution region of the Pt-Mn system :

$$\ln \gamma_{Mn} = 14.47\, X_{Mn} - 10.793 \qquad (11)$$

There is an excellent agreement between the linear regression of this work and the one from Rao an Gaskell[26]. Equation (11) permits the calculation of the limiting Henrian activity coefficient of manganese (γ^{o}_{Mn}) in Pt-Mn system as 2.05×10^{-5}, and the self interaction parameter of manganese, ϵ^{Mn}_{Mn} as 14.47 at 1500°C in dilute solutions. The γ^{o}_{Mn} value calculated in this work is also in excellent agreement with that provided by Rao and Gaskell[26]. Strong negative deviations from ideality were observed.

3.2 Activity of MnO in CaO-MgO-Al_2O_3-SiO_2-MnO slags.

Around 200 successful experimental runs were carried out in order to determine MnO activities in the slags at 1500°C. The Po_2 values varied from about 4.7×10^{-7} to 5.8×10^{-8} atom. The liquidus temperatures of all the 55 slag compositions were determined by Eric, Hejja and Stange[27] along with their electrical conductivity.

All the slags were found to be molten at temperatures less than 1400°C, and thus at 1500°C they would all form homogeneous liquid slags. The basicity ratio of the slags defined as (% CaO + % MgO)/%SiO_2 varied between 0.41 and 1.18.

The available experimental data on MnO activity was modelled by the use of neural nets utilizing
equation 12. The smoothing was done by Distance Weighted Least Squares (DWLS) method[28]. The neural net for expressing the activity of MnO as a function of the mole fractions of the slag components has 4 sigmoidal hidden nodes. Neural net weights as defined by equation 12 are collected in Table I.

Figure 1 gives a_{MnO} as neural net functions[8] of the basicity, % MnO in the slag and a CaO/MgO ratio of 1. The statistics for training the 150 data sets are R^2=0.96 for 130 degrees of freedom. For comparison Figure 2 presents an interpolation of the raw data indicating that the neural net model[8] has captured the functional relationships. It must be noted that this interpolation does not provide an equation, whereas the neural net does. Furthermore it is not possible to investigate the effect of the % CaO/%MgO ratio with this smoothing, which is possible with a neural net.

Figures 3 to 5 illustrate DWLS smoothing of raw data for a_{MnO}, γ_{MnO} and $\ln\gamma_{MnO}$ respectively as a function of the mole fractions of the slag components to show the trends rather than quantitative information. Figure 6 is a similar plot for $\ln\gamma_{MnO}$ where linear regression of the raw data is illustrated with 95% confidence limits. It is quite clear that a_{MnO}, γ_{MnO} and thus $\ln\gamma_{MnO}$ increases with increasing concentration of MnO and decreasing concentration of SiO_2. The effect of alumina is not clear, whereas the effects of CaO and MgO seem rather similar, they tend to increase both activity and activity coefficient of MnO as their concentrations increase. Figures 7 and 8 are three dimensional plots showing the DWLS smoothing of a_{MnO} and γ_{MnO} raw data respectively as a function of X_{CaO}/X_{SiO_2} ratio and X_{MnO} for all mole fractions of alumina and MgO. Figures 9 to 12 are the actual neural net modelling of the activity and activity coefficient of MnO. Figures 9 and 10 illustrate a_{MnO} as functions of X_{CaO}/X_{SiO_2} ratio and X_{MnO} for constant $X_{MgO} = 0.1$ and $X_{Al_2O_3} = 0.02$, and $X_{Al_2O_3} = 0.03$ respectively. For these two figures the statistics for training the 194 data sets were $R^2 = 0.97$ for 166 degrees of freedom. It is clear that a_{MnO} increases as its own concentration and X_{CaO}/X_{SiO_2} ratio increases.

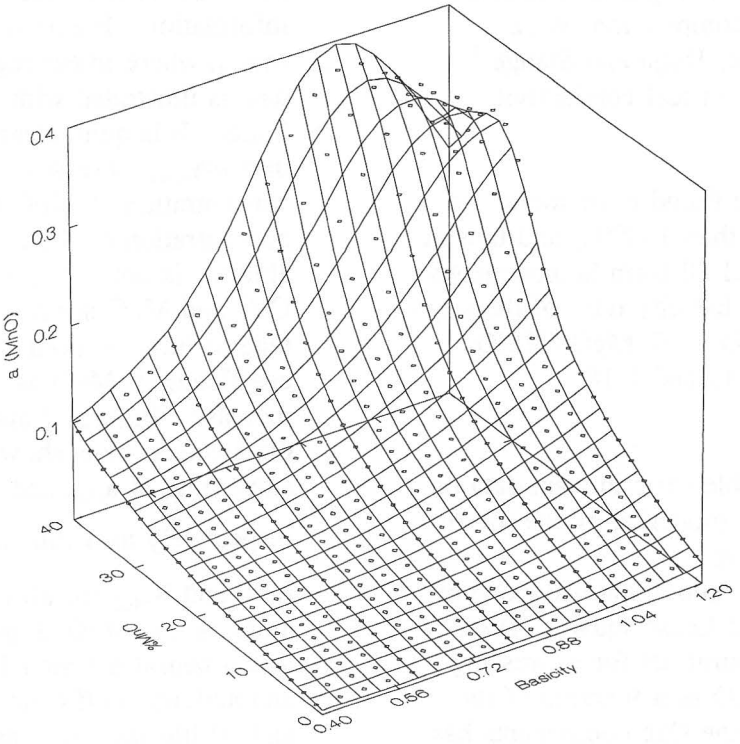

Figure 1 a_{MnO} as a neural net function of the basicity $= \dfrac{(\%CaO + \%MgO)}{\%SiO_2}$ and %MnO in the slag for $\dfrac{\%CaO}{\%MgO} = 1$

$$y=\frac{P25}{1+e^{-(P1+P2X_1+P3X_2+P4X_3+P5X_4+P6X_5)}}+\frac{P26}{1+e^{-(P7+P8X_1+P9X_2+P10X_3+P11X_4+P12X_5)}}$$

$$+\frac{P27}{1+e^{-(P13+P14X_1+P15X_2+P16X_3+P17X_4+P18X_5)}}+\frac{P28}{1+e^{-(P19+P20X_1+P21X_2+P22X_3+P23X_4+P24X_5)}} \quad (12)$$

where

$$X_1=\frac{X_{MnO}-0.0324}{0.3637}=\frac{X_{MnO}-Min\ value}{\max value}$$

$$X_2=\frac{X_{CaO}-0.0393}{0.3829},\ X_3=\frac{X_{MgO}-0.0046}{0.4955},$$

$$X_4=\frac{X_{SiO_2}-0.2533}{0.5877}$$

$$X_5=\frac{X_{Al_2O_3}-0.0134}{0.0508}\ and\ y=\frac{a_{MnO}-0.011}{0.364}$$

Table 1. Neural Net Weights as Defined by Equation 12

Label	Weights	Label	Weights	Label	Weights	Label	Weights
p1	-1.9366002 72812450	p8	-5.8465805 45817350	p15	2.25674700 6769990	p22	0.0225372 30852803
p2	4.65082551 4454860	p9	-4.0307864 91897640	p16	-0.4648528 91545478	p23	-.592493059 6153080
p3	-0.8219432 53199961	p10	-2.1477195 26270860	p17	4.80635460 8575110	p24	-2.6430479 77046420
p4	0.78664700 5584741	p11	13.6101128 47762400	p18	0.03028699 2016206	p25	3.9634046 18746080
p5	-4.2507454 00742890	p12	2.22517347 7549650	p19	-3.5940266 55949930	p26	-2.3709380 553221890
p6	-0.3802321 87740588	p13	1.14082406 0755000	p20	3.90162639 7884200	p27	2.3689630 34842840
p7	5.40263850 6648080	p14	-4.9133950 85511530	p21	0.69886217 5584405	p28	-7.2395059 52868250

Figures 11 and 12 show the functional dependence of the activity coefficient of MnO on X_{CaO}/X_{SiO_2} ratio and X_{MnO} for constant X_{MgO} = 0.1,

$X_{Al_2O_3}$ = 0.03 and X_{MgO} = 0.3,

$X_{Al_2O_3}$ = 0.02 respectively. For these two figures the statistics for training 194 data sets were R^2 = 0.92 for 166 degrees of freedom. Once again γ_{MnO} increases as X_{MnO} and X_{CaO}/X_{SiO_2} ratio increases, but as illustrated in figure 12, at relatively high concentrations of MgO, the increase in γ_{MnO} at low MnO concentrations is much more pronounced than at higher MnO concentrations as $X_{CaO}/_{SiO_2}$ ratio increases. An opposite behaviour is seen at low MgO concentrations as seen in Figure 11.

In general the result of this work are in good agreement with those of Warren[24]. However, it was found in this work that an increase in Al_2O_3 content of the slag would tend to increase the activity coefficient of MnO for a given X_{CaO}/X_{SiO_2} ratio or for a given basicity ratio. This is in contrast to Warren's[24] work where it was claimed that an increase in alumina would decrease the activity coefficient of MnO in highly basic slags. In this work such highly basic slags were not tested, and in more acidic slags employed here, it could be expected that Al_2O_3 may behave more like a basic oxide, and thus act as a network breaker, releasing free oxygen ions that can be associated with Mn^{2+} ions resulting in an increase in the activity and activity coefficient of MnO. An opposite behaviour by Al_2O_3 in highly basic slags - like those of the previous study[24] - could be expected.

4. CONCLUSIONS

1) There is a good agreement between the present and the previous study on the activity-composition relations in solid Pt-Mn alloys at 1500°C and $\ln\gamma_{Mn}$ has been presented as a simple linear equation.

2) Activity of MnO in CaO-MgO-SiO_2-Al_2O_3-MnO slags pertinent to ferromanganese and silicomanganese smelting has been measured and modelled by neural nets.

3) Activity and activity coefficient of MnO in the slag increases with its concentration and with increasing basicity ratio and X_{CaO}/X_{SiO_2} ratio.

4) An increase in Al_2O_3 content of the slag tends to increase the activity and activity coefficient of MnO for a given basicity or X_{CaO}/X_{SiO_2} ratio.

ACKNOWLEDGEMENTS

The authors are grateful to Council for Mineral Technology (Mintek) and Ferro Alloy Producers Association (FAPA) of South Africa for financial assistance to undertake this research.

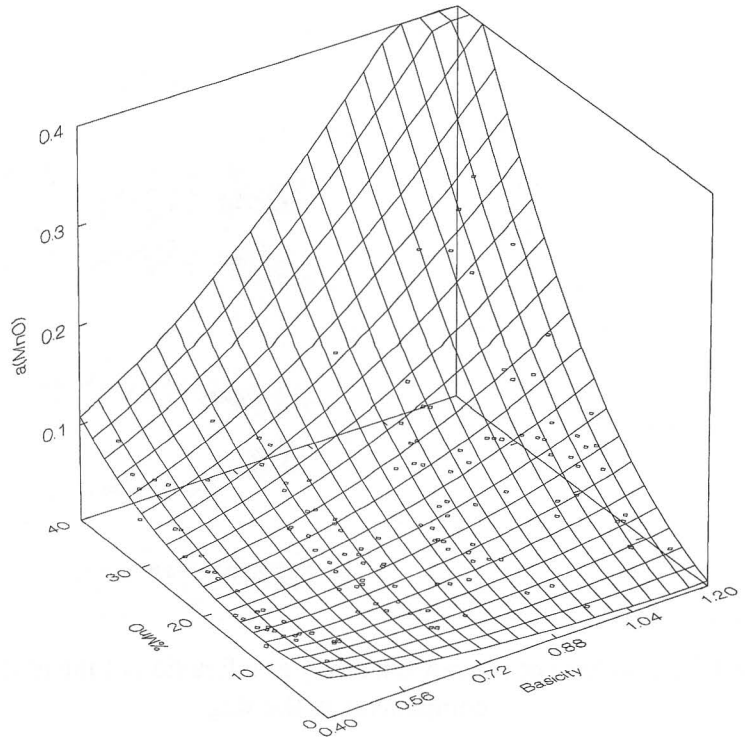

Figure 2 a_{MnO} as a DWLS smoothing of the basicity $= \dfrac{(\%CaO + \%MgO)}{\%SiO_2}$ and %MnO for all $\dfrac{\%CaO}{\%MgO}$

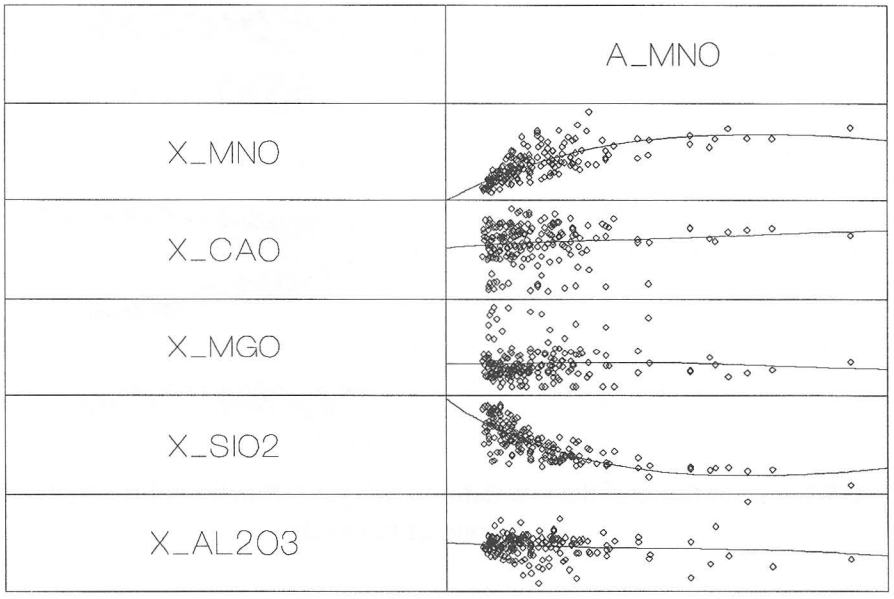

Figure 3 DWLS smoothing of the raw data for a_{MnO} as a function of the mole fractions of the components in the slag

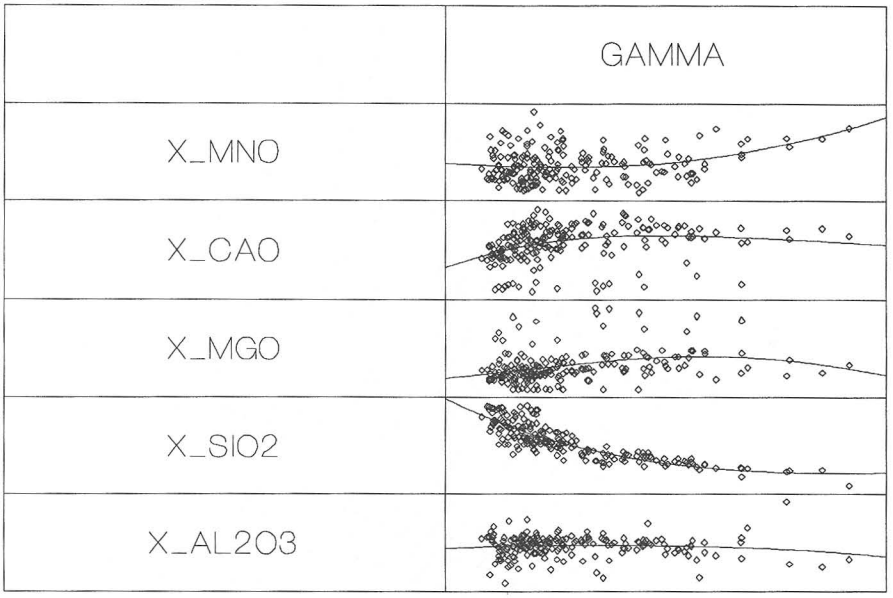

Figure 4 DWLS smoothing of the raw data for γ as a function of the mole fractions of the components in the slag

A multi-linear regression of the data produces a R^2=0.7.

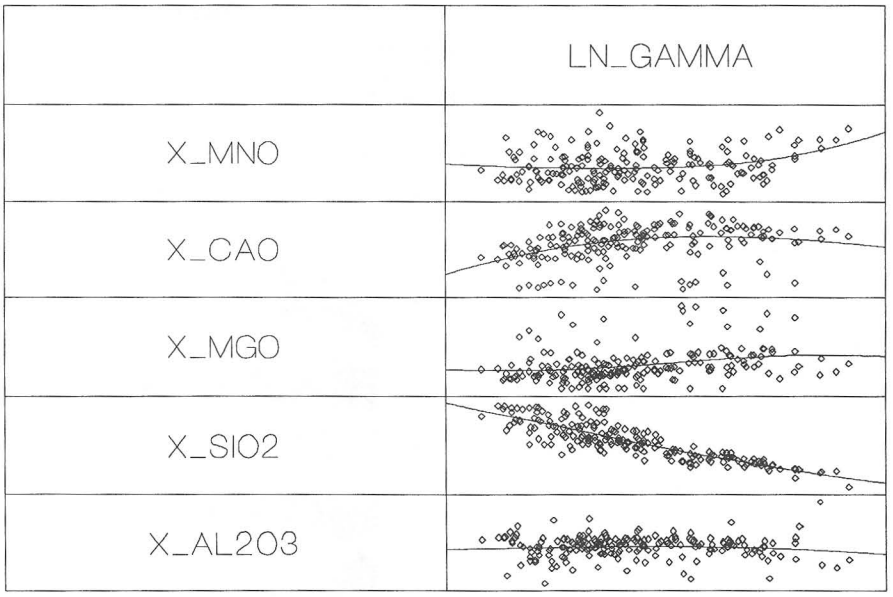

Figure 5 DWLS smoothing of the raw data for ln(γ) as a function of the mole fractions of the components in the slag

A multi-linear regression of the data produces a R^2=0.786.

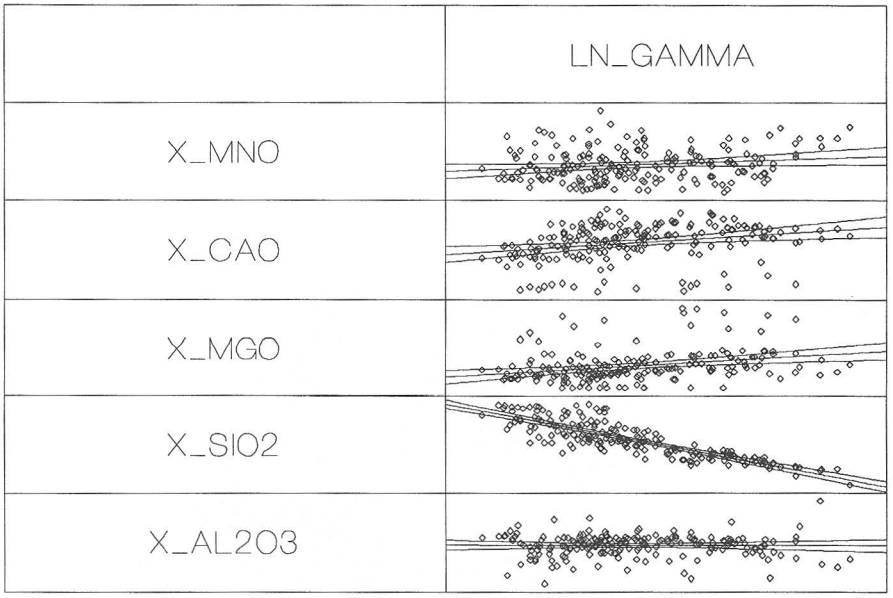

Figure 6 Linear regression of the raw data for ln(γ) as a function of the mole fractions of the components in the slag with 95% confidence limits included

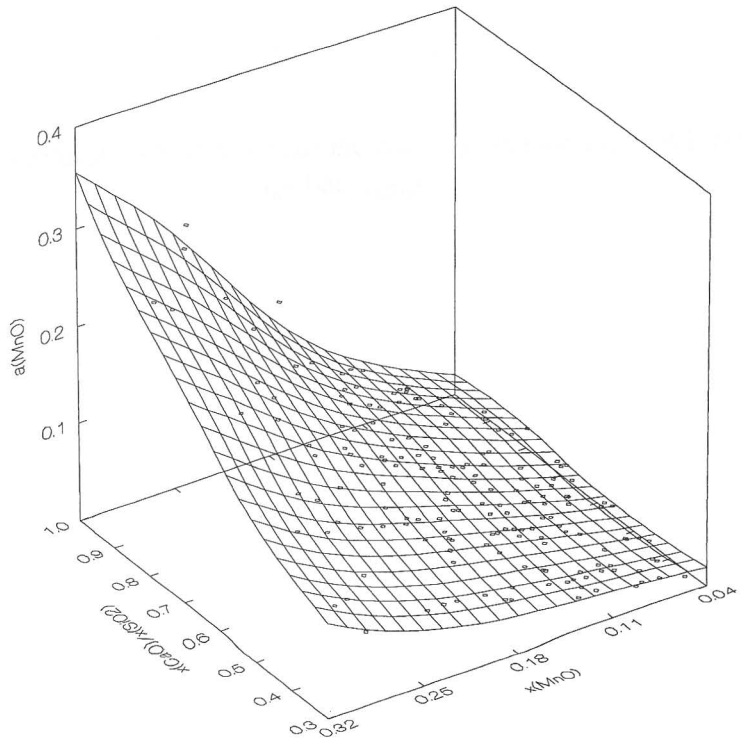

Figure 7 DWLS smoothing of a_{MnO} raw data as a function of x_{CaO}/x_{SiO2} and x_{MnO} for all x_{Al2O3} and x_{MgO}

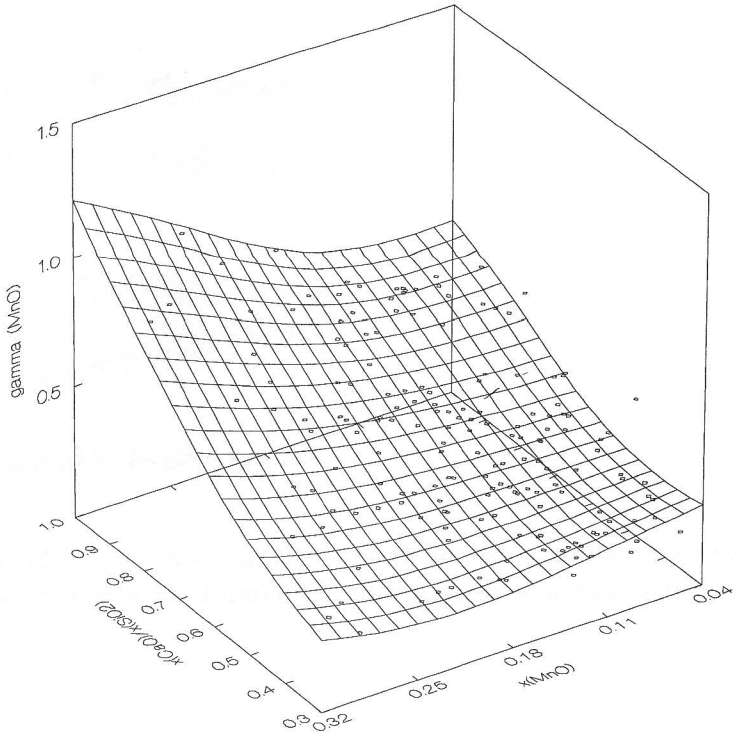

Figure 8 DWLS smoothing of γ_{MnO} raw data as a function of x_{CaO}/x_{SiO2} and x_{MnO} for all x_{Al2O3} and x_{MgO}

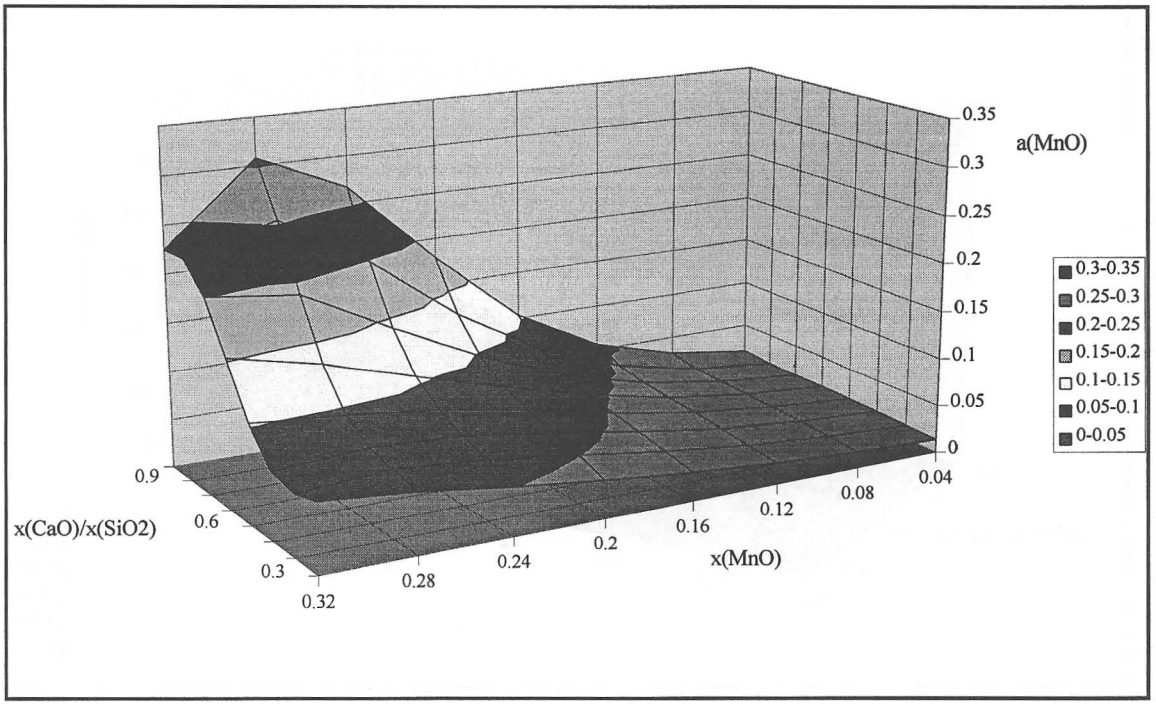

Figure 9 A neural net function of a_{MnO} as a function of x_{CaO}/x_{SiO2} for x_{MgO}=0.1 and x_{Al2O3}=0.02

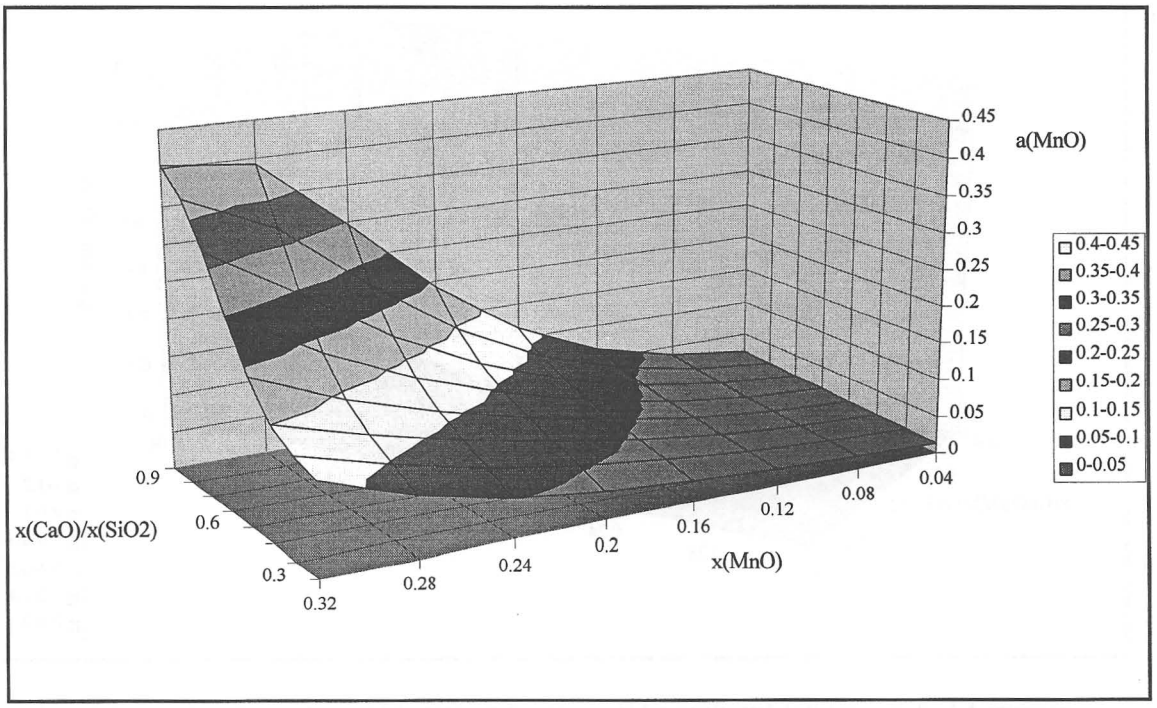

Figure 10 A neural net function of a_{MnO} as a function of x_{CaO}/x_{SiO2} for x_{MgO}=0.1 and x_{Al2O3}=0.03

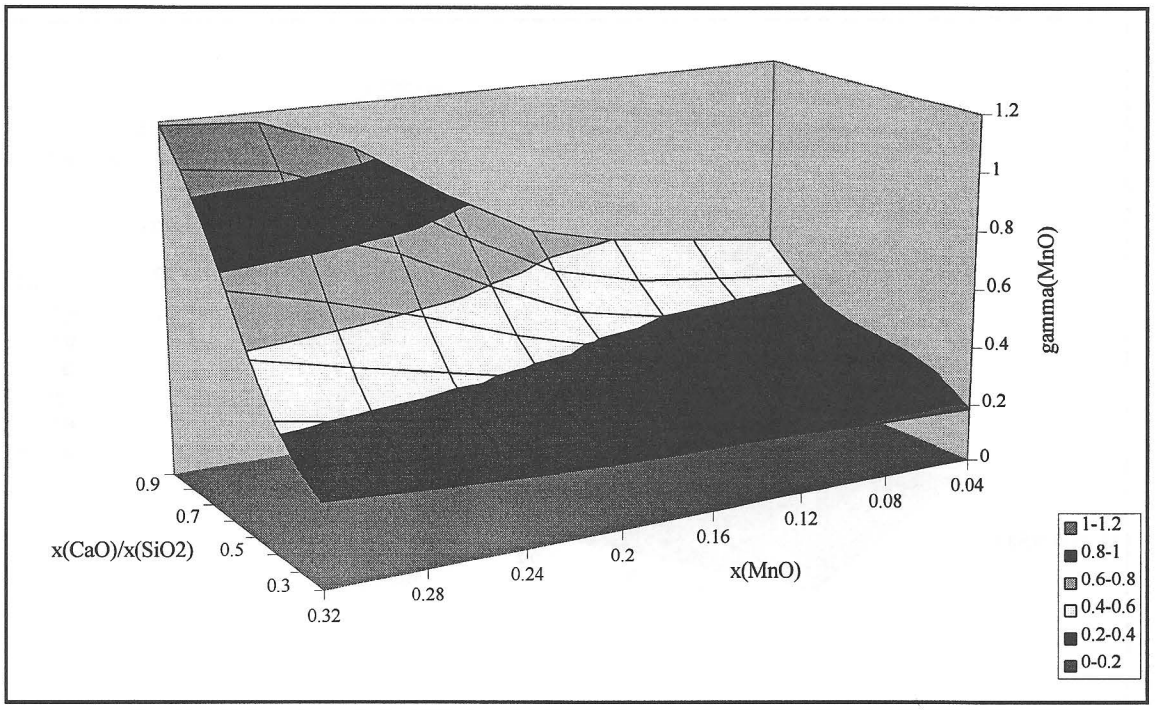

Figure 11 A neural net function of γ_{MnO} as a function of x_{CaO}/x_{SiO2} for x_{MgO}=0.1 and x_{Al2O3}=0.03

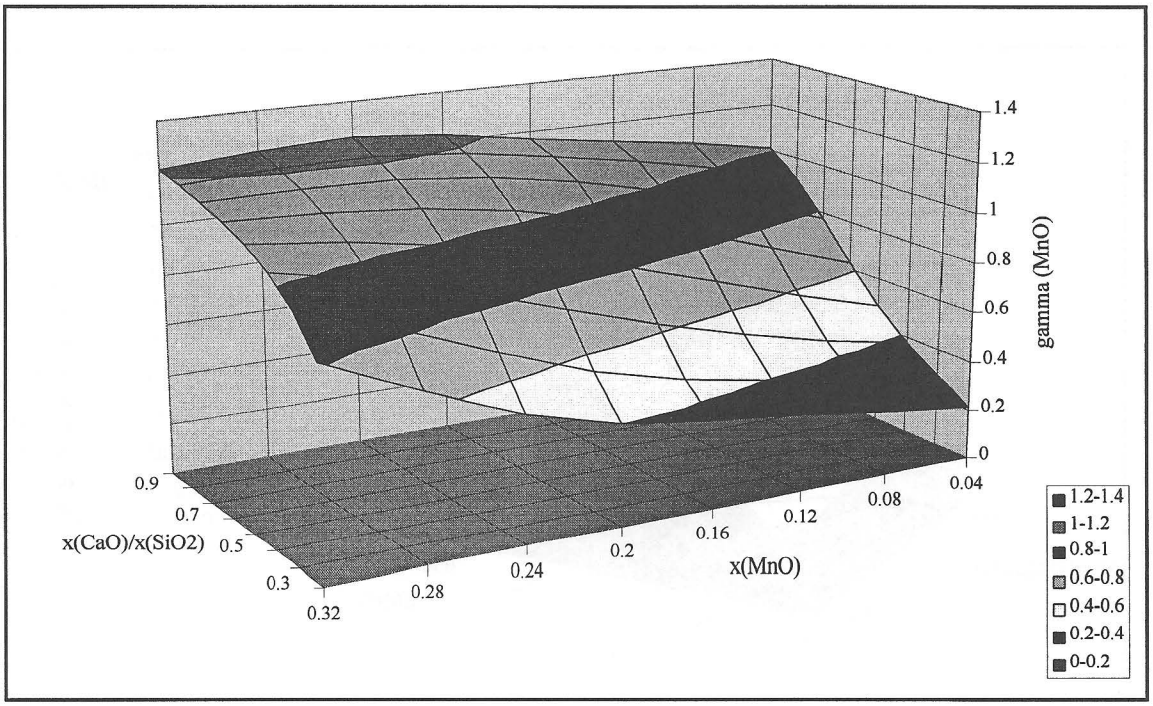

Figure 12 A neural net function of γ_{MnO} as a function of x_{CaO}/x_{SiO2} for x_{MgO}=0.3 and x_{Al2O3}=0.02

REFERENCES

1. R.P. Lippmann, "An Introduction to computing with neural Nets," IEEE ASSP Magazine, vol. 4, No. 2, 1987, pp. 4 - 21.

2. D.E. Rumelhart, G.E. Hinton and R.J. Williams, "Learning Internal Representation by Error Propagation," Parallel Distributed Processing, Vol. 1, MIT Press, Cambridge, Massachusetts, 1986, pp. 318 - 362.

3. M.J.D. Powell, "Restart procedures for the Conjugate Gradient Method," Mathematical Programming, Vol. 12, 1977, pp. 241 - 254.

4. W.H. Press et al, The Art of Computing, Cambridge University Press, Cambridge U.K., 1989.

5. E. Barnard and R.A. Cole, " A Neural Net Training Program Based on Conjugate-Training Optimisation." Technical Report No. CSE 89 014, Carnegie-Mellon University, Pittsburgh, USA, 1989.

6. K. Hormik, M. Stinchcombe and H. White, "Multilayer Feedforward Networks are Universal Approximators," Neural Networks, Vol. 2, 1989, pp 359 - 366.

7. M.A. Reuter, T.J. Van der Walt and J.S.J. van Deventer, "Modelling of Equilibrium Processes in Pyrometallurgy by Neural Nets," Metallurgical Transactions B, Vol. 23b, 1992, pp. 643 - 650.

8. M.A. Reuter, "Hybrid Neural Net Modelling in Metallurgy," Metallurgical Processes for Early Twenty-First Century, Ed. H.Y.Sohn, The Minerals, Metals and Materials Society, Warrandale, PA, 1994, pp. 907 - 927.

9. J. Friedman, "Multivariate Adaptive Regression Splines," The Annals of Statistics, Vol. 19, No. 1, 1991, pp. 141.

10. M.A. Kramer, "Nonlinear Principal Component Analysis Using Auto associative Neural Networks," AIChE Journal, Vol. 37, No. 2, 1991, pp 233 - 243.

11. F.P. Glasser, "The System MnO-SiO_2," American Journal of Science, vol. 256, June 1958, pp. 398 - 412.

12. W.J. Rankin, "Silica Solubility and the Activity of MnO in MnO-SiO_2 Slags," Metallurgical Transactions B, Vol 9B, 1978, pp. 726-728.

13. K.P. Abraham. M.W. Davies and F.D. Richardson, "Activities of Manganese Oxide in silicate melts," J.I.S.I, Vol. 196, 1960, pp. 82 - 89.

14. S.R. Mehta and F.D. Richardson, "Activities of Manganese Oxide and Mixing Relationships in Silicate and Aluminate Melts," J.I.S.I., Vol. 203, 1965, pp. 524 - 528.

15. J. Chipman, J.B. Gero and B. Winkler, "The Manganese Equilibrium in Simple Oxide Slags," Trans. of the Metallurgical Society of AIME, Vol 188, 1950, pp. 341 - 345.

16. H.B. Bell, "Equilibrium between FeO-MnO-MgO-SiO_2 Slags and Molten Iron at 1550°C," J.I.S.I., Vol. 201, 1963, pp. 116 - 121.

17. W.A. Fischer and H.J. Fleischer, "The Manganese Distribution between Iron melts and FeO Slags in MnO Crucibles in the Temperature Range 1520° to 1770°C," Archive fur das Eisenhuttenwesen, Vol. 32, 1961, pp 1 - 10.

18. E.T. Turkdogan and J. Pearson, "Activities of constituents of Iron and Steelmaking Slags, Part II - manganous Oxide," J.I.S.I., Vol. 175, 1953, pp. 393 - 398.

19. H.L. Bishop, N.J. Grant and J. Chipman, "The Activity Coefficient of MnO and FeO in Open-Hearth Slags," Transactions of the Metallurgical Society of AIME. Vol. 212, 1958, pp 890 - 892.

20. E.W. Tiler and L.W. Darken, "Equilibrium Between Blast Furnace Metal and Slag as Determined by Remelting," Journal of Metals, Vol. 194, 1952, pp. 253 - 257.

21. E.T. Turkdogan, "Silicon and Manganese Reactions in Ferromanganese Blast Furnace Processes," J.I.S.I., Vol 182, 1956, pp. 74 - 79.

22. W.J. Rankin and J.B. See, "The Slag-Metal Equilibrium and the Activities of Slag and Metal Components in the Production of High Carbon Ferromanganese," National Institute for Metallurgy Report, No. 1959, Randburg, South Africa, 1978.

23. B.K.D.P. Rao and D.R. Gaskell, "The Thermodynamic Activity of MnO in Melts Containing SiO_2, B_2O_3 and TiO_2," Metallurgical Transactions B, Vol. 12B, 1981, pp. 469 - 477.

24. G.F. Warren, "Measurement of the Activities of Manganese (II) Oxide in Slags Associated with the Production of High Carbon Ferromanganese," M.Sc(Eng) Dissertation, University of the Witwatersrand, Johannesburg, South Africa, 1972.

25. M.W. Davies and F.D. Richardson, "The Non-Stoichiometry of Manganous Oxide," Transactions of the Faraday Society, vol. 55, 1959, pp. 604 - 610.

26. B.K.P.D Rao and D.R. Gaskell, "The Thermodynamic Activity of Manganese in Pt-Mn Alloys in the Temperature Range 1300° - 1600°C, Metallurgical Transactions. Vol. 12A, 1981,. pp. 207 - 211.

27. R.H. Eric, A.A. Hejja and W. Stange, "Liquidus Temperature and Electrical Conductivities of Synthetic Ferromanganese Slags," Minerals Engineering, Vol. 4, 1991, pp. 1315 - 1332.

28. SYSTAT for windows : Statistics, Version 5 Edition, Systat. Inc. Evanston, IL, 1992, pp 750.